A98-31538

ICAS-98-3,2,3

A STUDY OF VORTEX BREAKDOWN ON PITCHING DELTA WINGS USING HIGH RESOLUTION PRESSURE MEASUREMENTS.

By

M.L. Jupp, F.N. Coton, R.B. Green, R.A.McD. Galbraith

Department of Aerospace Engineering
University of Glasgow, Glasgow, G12 8QQ, U.K.

Abstract

This paper describes and presents results from wind tunnel tests conducted on two 60° delta wings at a root chord Reynolds number of 2.7×10^6. In these tests, the wings were instrumented with 192 miniature pressure transducers which, in conjunction with a powerful multi-channel data-logging system, allowed the distribution of time-varying surface pressures to be measured at high temporal resolution. The wings differed only in the shape of the nose section. It is shown that analysis of root-mean-square (RMS) pressure on the leeward surface of each wing highlights significant differences in the formation, position and movement of the vortical structures on the two planforms with increasing pitch rate. The relationship between these observations and previously observed behavioural characteristics of vortex breakdown is then discussed.

Nomenclature

c	root chord
k	reduced pitch rate ($\omega c/2U$)
s	local semi-span
s_{te}	trailing-edge semi-span
U	mean freestream velocity
x	chordwise distance from apex
x/c	non-dimensional chord position
y	spanwise distance from wing centreline
y/s	non-dimensional span position
z	distance measured normal to the leeward surface
z/s	non-dimensional height above the leeward surface
$2s_{te}$	trailing-edge span
α	angle of incidence (deg)
ω	nominal pitch rate ($rads^{-1}$)

Introduction

The flow structures on the leeward surface of sharp-edged delta wings have been the subject of research since the early 1950's. It is now well known that the flow is dominated by a pair of primary vortices extending rearwards from the wing apex. The location and height above the wing of each centreline is chiefly dependent on angle of attack, the sweep angle and the shape of the leading-edge [1]. Each primary vortex is responsible for the formation of a secondary smaller vortex structure rotating in opposition to its primary parent.

As may be expected, the primary vortices dominate the lift response of the wing and allow the generation of lift to continue at angles of incidence beyond the recognised stall condition of conventional wings. However, at some value of incidence and at some point along the vortex core, a sudden transformation takes place causing the axial velocity of the flow to stagnate and the vortex to break down into large scale turbulence. This phenomenon of vortex 'burst' has greatly interested researchers since it was apparently first observed by Elle [2] in 1960 and defined by Lambourne & Bryer [1] in 1962.

Experimental research programmes in this area [1,2,3,4&5] have made extensive use of flow-visualisation and qualitative techniques to clarify the physical mechanisms involved in the formation, maintenance and eventual breakdown of vortical flows. By and large, these investigations have been confined to static cases although some studies have focused on the effect of pitch rate and oscillation frequency, on the vortex breakdown phenomenon [6,7,8,9&10].

A more limited number of researchers [11,12&13] have concentrated their efforts on capturing

features of the upper surface pressure distribution on a series of stationary, and pitching wings. It has been successfully shown that there is consistent hysteretic behaviour associated with the pressure distribution on pitching wings when compared with the stationary wing at a given angle of attack. In a similar manner to vortex breakdown, the phase lag in pressure measurements appears to be chiefly dependent on pitch rate. In many cases however, the studies have been compromised by the limitations of the test set-up used. Small numbers of transducers and/or relatively low sampling rates have resulted in low spatial and temporal resolutions which make vital components of the flow structure difficult to resolve and explain.

This paper describes a series of experiments on two delta wing planforms with sharp leading edges. In these tests, which were carried out in the Handley-Page wind-tunnel facility at Glasgow University, a fully-automated data acquisition system was used to obtain unsteady surface pressure measurements at high temporal and spatial resolution. The high temporal resolution of the measured data allowed a detailed analysis of the fluctuation components within the signals obtained from high speed pitching cases to be conducted. The focus of this paper is on the use of this type of analysis to detect vortex breakdown during ramp up motions. In this way, the effect which rounding the wing apex has on vortex behaviour and in particular, the sensitivity of the progression of vortex breakdown to pitch rate, could be assessed.

Experimental Method

Model Design and Construction.

The basic delta wing used in the test programme was machined from a solid block of aluminium. It had an 800mm root-chord, and a sweep angle of 60°. This gave an aspect ratio of 2.31 and a trailing edge span ($2s_{te}$) of 923.8mm. The wing had a flat leeward surface, a highly contoured windward surface, (giving a thickness ratio of 9.0%) and bevelled edges on the windward side to produce sharp leading and trailing edges. The model was designed to accommodate 192 Kulite Type CJQH-187 differential pressure transducers located primarily on the starboard side of each surface. The shape of the windward surface and the location of the leeward surface transducers is shown in Figure 1.

The model was constructed such that the standard nose-section could be removed and replaced with a rounded nose-section, (Figure 2). The rounded nose had a radius of 50mm and had the effect of reducing the root chord by 6.25%. It had a bevelled leading-edge similar to its standard counterpart which provided a unique opportunity to investigate the effect of the apex geometry on vortex formation and breakdown.

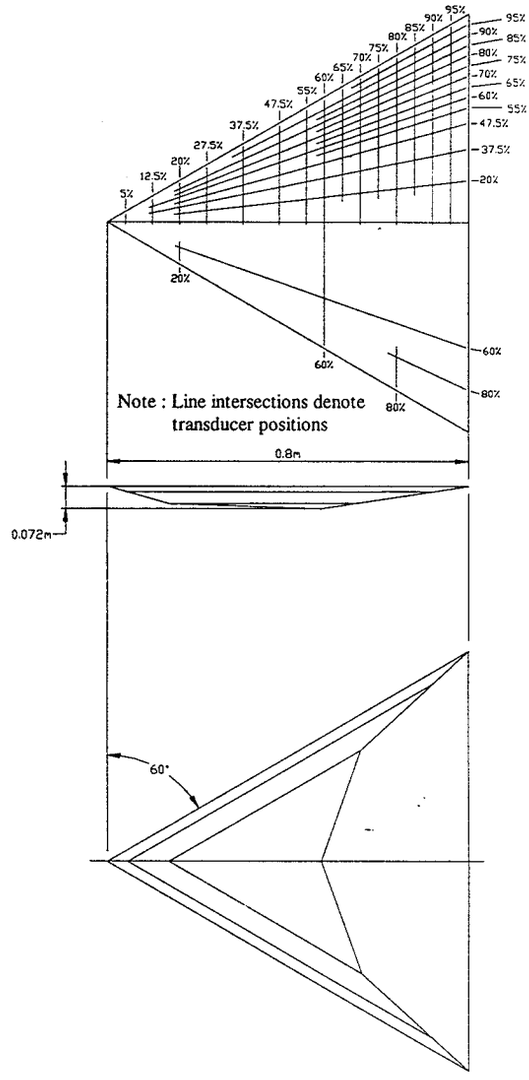

Figure 1 - The Delta Wing Model Leeward Surface Transducer Positions & Windward Surface Shape

The Wind-Tunnel Facility.

The tests were conducted in the Department's Handley-Page wind-tunnel facility. This is a closed return type wind tunnel with an octagonal test section measuring 2.13m by 1.61m (working area = 2.667m^2), which gave a model-span to tunnel width ratio of 43.4% and a model blockage (not including strut fairings)

of 1.25% to 9.27% over the incidence range $0° \leq \alpha \leq 42°$. The model was mounted leeward side up, and was supported by three vertical struts, one placed at the quarter chord position and two at the trailing edge. The forward strut was rigidly fastened to a support structure mounted on the concrete floor below the wind tunnel. The two rear struts were connected to a hydraulic actuation mechanism situated below the tunnel floor.

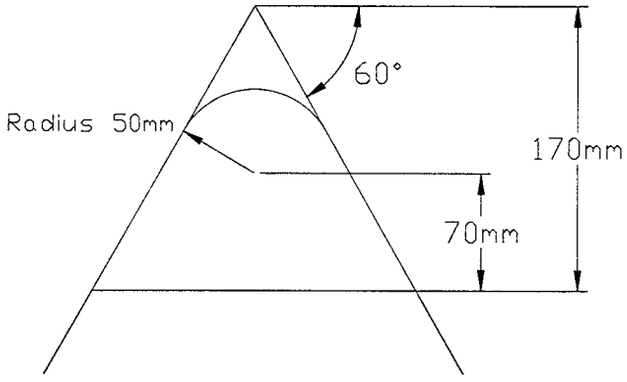

Figure 2 - The Delta Wing Model Round-Nosed Section

The model was pitched about the quarter chord position by vertical displacement of the two rear struts using a Parker 2H Series linear hydraulic actuator. This system used a high-response proportional-directional control valve with a E200-595 PID analogue closed loop controller, which could deliver a maximum thrust of 17.0KN during extension and 6.53KN during retraction at a piston speed of 1.1m/s. An angular displacement transducer mounted at the pitch location was used to provide the feedback signal, which was also used for recording the instantaneous angle of attack. The required motion profile was provided by an AMSTRAD 1512 microcomputer equipped with an Analog Devices RT1815 multi-function input/output board. The required output function was digitised into equal time steps and the frequency was controlled using interrupts on the AMSTRAD microcomputer.

The Data Acquisition System.

Data acquisition was carried out by a PC equipped with a 486 processor, programmed using TEAM 256 software. The PC was configured and interfaced with propriety Bakker Electronics BE256 modules which provided the necessary analogue to digital conversion. The system had 200 channels, each capable of sampling at 50kHz. The channels not taken up by transducers were used to sample temperature, barometric pressure, reference dynamic pressure and model incidence. The signals from each transducer were delivered to a specially designed signal conditioning unit of modular construction, and each module contained its own control board. The control board was capable of automatic offset and gain adjustment by sampling the minimum and maximum output of each transducer during each run and adjusting the gains automatically as required.

Experimental Procedure.

For the static tests, the wing was set at a starting incidence of -5°. The wing was then pitched up in 1° increments to +42°. A suitable period was allowed prior to data collection at each incidence and the pressure data were then sampled at a frequency of 2.0kHz for a period of 1s. The total data set was divided into three 'runs' each covering an arc of 16°, giving a data set of 32000 samples per run.

For the ramp tests, the wing was set at a starting incidence of -5° and pitched-up at a constant pitch rate over an arc of 45°. Some 8000 samples of pressure data were collected during each cycle and the ramp motion was repeated over several cycles. Data from four cycles of motion were recorded at each pitch rate to give a total of 32000 samples over the range of incidence under consideration.

The mean free stream velocity for all tests was measured at $50ms^{-1}$, which gave a Mach number of 0.162 and a Reynolds number of 2.7×10^6 based on root chord.

Results

Static Cases

For a given transducer, the pressure data at each angle of incidence were non-dimensionalised and averaged to produce a value of mean C_P. A study of the mean C_P data revealed the growth of a localised 'suction' ridge on the leeward surface of each wing extending, from the apex area towards the trailing edge. For both wing configurations, this ridge first became apparent in the data at an incidence of 2°. Figure 3 shows a series of contour plots indicating the mean C_P distribution on the leeward surface of the sharp-nosed and round-nosed wings at various incidences. The plots are indicative of a

general trend. That is, for all angles of incidence the magnitude and localisation of the suction ridge (1) were at a maximum towards the apex of the wing, with a decrease in magnitude and a broadening of the ridge towards the trailing edge.

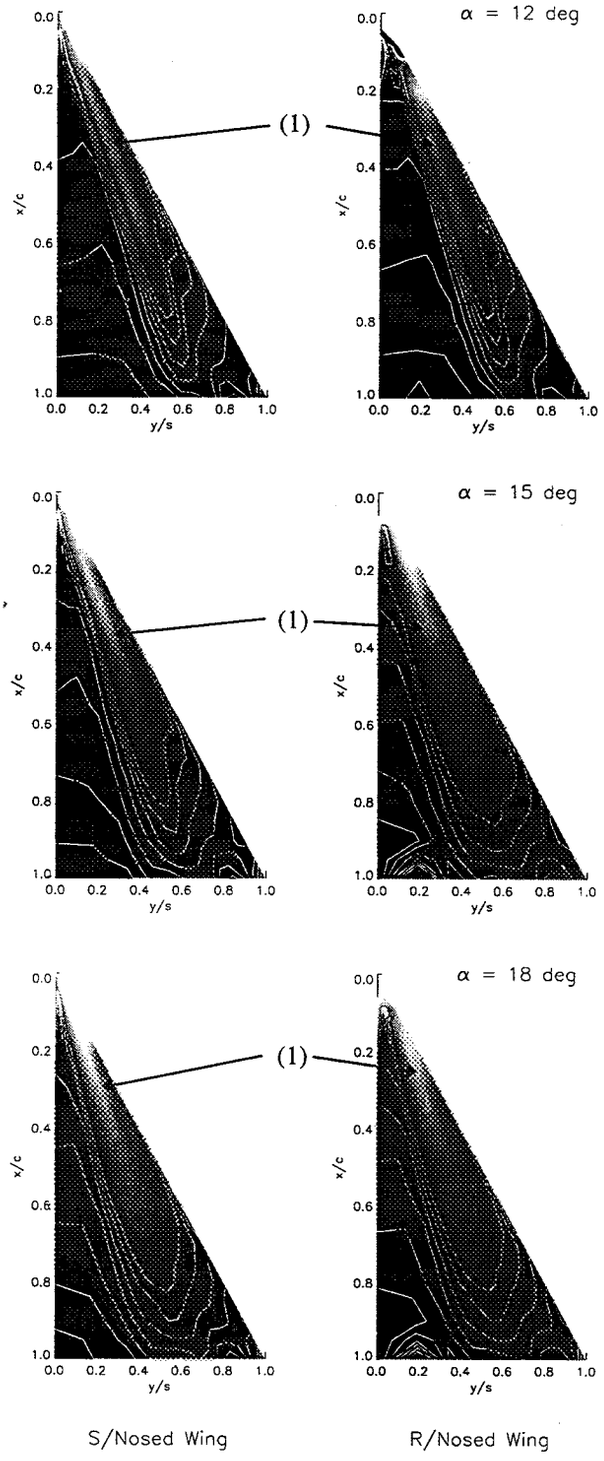

Figure 3 - Mean C_P distributions on two delta wing planforms at three angles of incidence.

Similarly, the ridge increased in magnitude and tended to move inboard as the incidence of the wing was increased. These findings were in keeping with the results presented previously by Parker [14], Jarrah [15] and Thompson et al [13]. Previous work [14] has shown that this region of high negative C_P corresponds more or less to the location above the wing of the centreline of the primary vortex core. On the sharp-nosed wing, this ridge emanates from the apex of the wing. On the round-nosed wing there is a region of low pressure at the apex but the suction ridge originates at a distance from the apex along the leading-edge at approximately x/c = 0.1. With an increase in incidence however, the origin of the ridge on the round-nosed wing moves upstream, reaching the apex at an incidence of 20° (not shown). The spanwise position of the vortex at the trailing edge is similar in both cases. To maintain this trailing-edge position at small incidences, the round-nosed vortex follows an increased angle relative to the leading-edge. At all incidences for both wing configurations, the width of the suction ridge is very similar.

In addition to the study of the mean C_P distribution, the root-mean-square (RMS) of the pressure deviations around the mean were examined for both wing planforms at each angle of incidence. Figure 4 shows a series of contour plots of the RMS pressure distribution on the leeward surfaces of the two wings at incidences of 6°, 8° and 10°. Examination of the distribution on either wing shows the growth of a region of high RMS pressure in the form of a ridge located along a ray from the apex area towards the trailing edge located somewhat inboard of the peak suction ridge. This region of high RMS pressure was previously observed by Woods & Wood [16] in their work on novel planforms. On the sharp-nosed wing, the region of high RMS pressure emanates from the apex of the wing whereas on the round-nosed wing, the origin of the high RMS region is not so well defined. For both wing planforms the initial appearance of this high RMS pressure region occurs at an incidence of 1°. Like the mean C_P distribution, the region of high RMS grows in strength with an increase in incidence, but unlike the mean C_P distribution its strength does not diminish with distance from the wing apex. At the low angles of incidence shown in Figure 4, the region of high RMS can be seen to begin to split into two. The 'primary' region (1) extends from the apex to the trailing edge whereas a 'secondary' region (2), which forms as

incidence is increased, is seen as a branch of the primary emanating downstream of the apex and terminating short of the trailing edge.

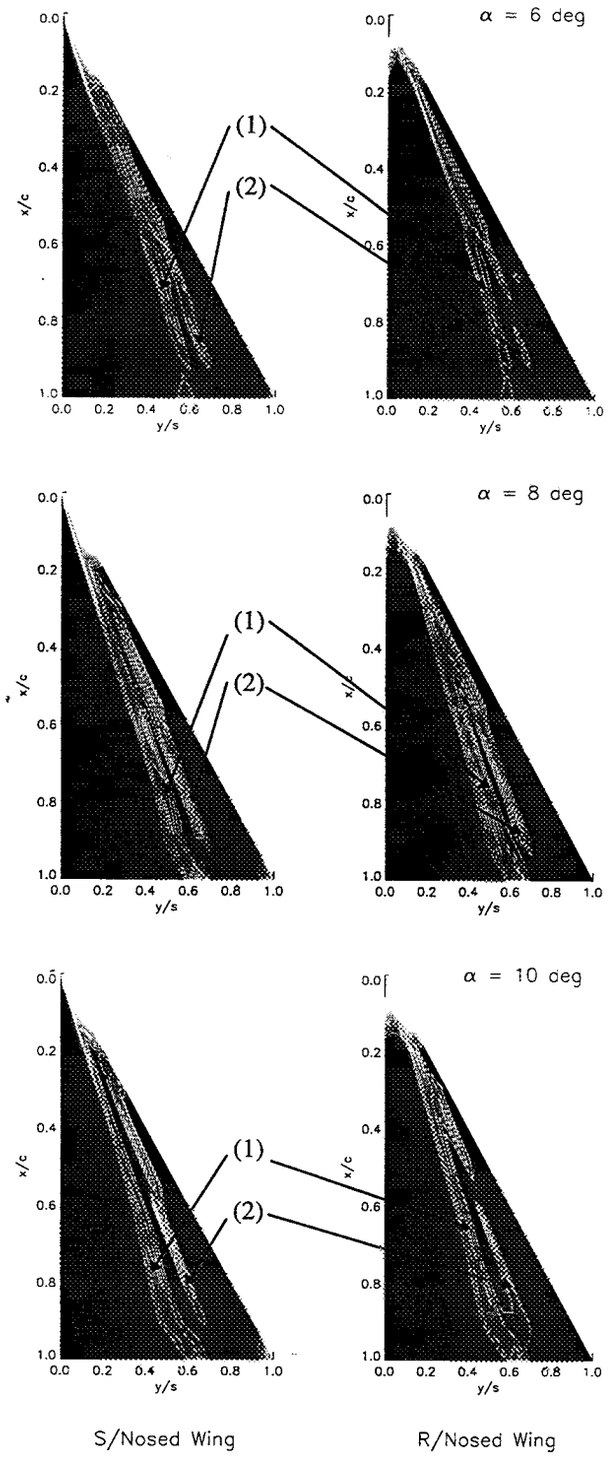

Figure 4 - RMS pressure distributions on two delta wing planforms at 6°, 8° & 10° incidence

A series of contour plots of the RMS pressure distribution on the leeward surface of each wing at three higher angles of incidence (12°, 15°,and 18°) are shown in Figure 5. At 12° incidence, it can be seen that the secondary branch of high RMS pressure first shown in Figure 4 is still apparent (1) although it has begun to fragment. At 13°(not shown), the secondary region of high RMS pressure on the round-nosed wing was seen to have all but disappeared, although on the sharp-nosed wing the same feature was discernible up to 15°.

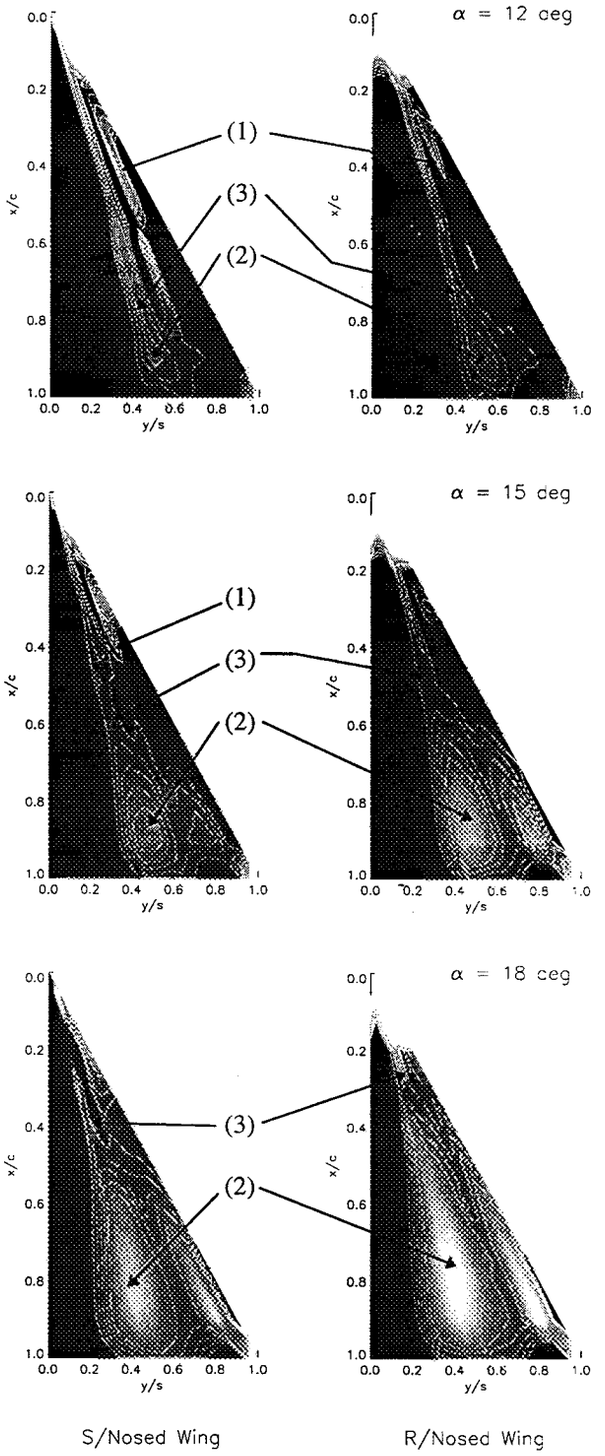

Figure 5 - RMS pressure distributions on two delta wing planforms at 12°, 15° & 18° incidence

More significantly, an additional peak of high RMS pressure is forming on the ridge of the primary region at a point close to the trailing edge (2). Careful scrutiny of all contour plots revealed that this additional peak first appeared at this location on both wings at an incidence of 11° (not shown). The significant features accompanying the appearance of the additional peak are a 'waisting' of the above-described ridge upstream of the peak centre (3) followed by a significant expansion towards the peak. The narrowest part of the waist corresponds to the minimum in a small localised trough of RMS pressure which occurs before the rapid increase towards the peak.

As the incidence increases further, the additional peak of high RMS pressure expands in all directions and the waist moves upstream. The principle differences in the RMS pressure distribution of each wing configuration is the speed at which the additional peak expands and the waist moves. In the case of the round-nosed wing, the 'apex' of the additional peak of high RMS pressure appears earlier and moves faster toward the apex of the wing. At 18° in either case, it is possible to detect the beginning of the upstream movement of the centre of the peak but this occurs much more slowly than either the expansion of the high RMS pressure peak or the movement of the waist

Pitching Cases

On both planforms there was an increasing delay in the formation of the previously observed suction ridge with an increase in pitch rate. A series of contour plots of the instantaneous C_P distribution on the leeward surface of each planform at three reduced pitch rates (k = 0.015, 0.03, and 0.053) are shown in Figure 6 for an incidence of 6°. Here, the suction ridge is seen to originate at the leading-edge rather than the apex of the wing. As incidence increased further however, the origin of the suction ridge on the sharp-nosed wing was seen to move upstream, reaching the apex at 8° regardless of pitch rate. On the round-nosed wing at a pitch rate of k = 0.015, the origin of the suction ridge remained stationary at x/c = 0.15, eventually beginning its move upstream at 22°, reaching the apex at 25°. At the higher pitch rate of k = 0.053, the origin moved upstream to x/c = 0.15 over the incidence range 5° - 9° where it remained stationary until 27°. After which it moved upstream, reaching the apex at 29°.

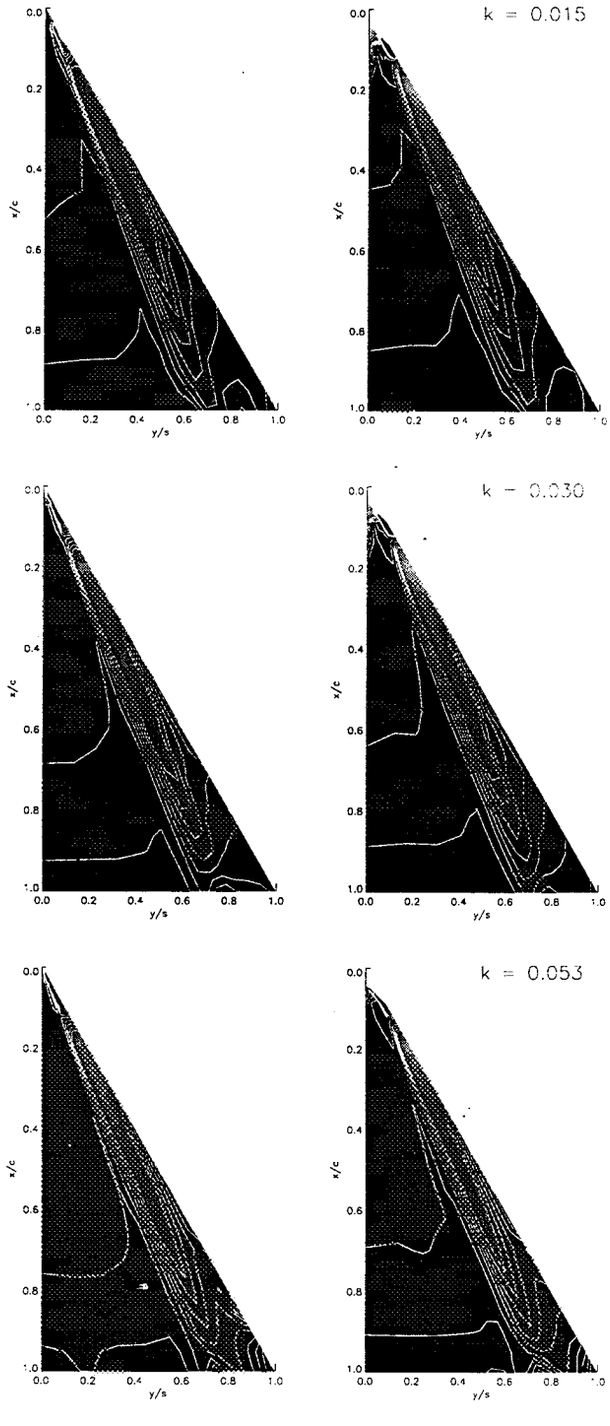

Figure 6 - Instantaneous C_P distributions on two pitching delta wing planforms at 6° incidence

Another interesting feature of the results is the effect of pitch rate on the spanwise location of the suction ridge. Figure 6 shows that the suction peak region, having originated on the leading-edge rather than the apex of the wing, tended to remain further outboard with

increasing pitch rate than the static cases shown in Figure 3. This trend continued throughout the incidence range overcoming the general trend for the vortex core to move inboard with an increase in incidence.

The high temporal resolution of the data provided the opportunity to study the RMS pressure distribution in pitching cases. This involved obtaining a trend line by applying a linear best-fit through the signal for a given transducer over an incidence range of one degree. The RMS value at the mid-range incidence was then calculated on the basis of the fluctuations around this trend line. During the pitch up, the primary ridge of high RMS pressure previously described for the static cases and shown in Figure 4 (1) was also apparent. This first appeared in all pitching cases at an incidence of 1°. Like the previously described suction ridge, the primary ridge of high RMS pressure was located progressively further outboard for a given incidence as pitch rate was increased.

For the round-nosed wing at a reduced pitch rate of k = 0.015, the secondary region of high RMS pressure (Figure 4 (2)) first appeared at an incidence of 4°. In the case of the sharp-nosed wing this feature was not apparent until 6°. The general trend for both wings at all pitch rates was for the appearance of the secondary region of high RMS pressure to be delayed until a higher incidence with increasing pitch rate.

At all pitch rates, an additional peak of high RMS pressure appears near the trailing edge of the sharp-nosed wing at an incidence of 13°. The same feature appeared on the round-nosed wing at a higher incidence of 14°. At first glance, the form of this additional peak appeared to be similar to that described for the static case and shown in Figure 5 (2). However, with a further increase in incidence the size of the additional peak tended to expand and then contract in a random manner, whilst its centre remained stationary near the trailing edge. Interestingly, the waisting of the RMS pressure contours previously described for the static case and shown in Figure 5 (3) was not apparent.

Figure 7 shows a series of contour plots of the leeward surface RMS pressure distributions for both wings at three reduced pitch rates (k = 0.015, 0.03 and 0.053) at an angle of incidence of 26°. Figure 7 indicates two predominant trends. The sharp-nosed wing lags its round-nosed counterpart in terms of the upstream movement and expansion of the centre of the additional peak of high RMS pressure (1). Similarly, both planforms exhibit a delay in the movement of the same features with increasing pitch rate.

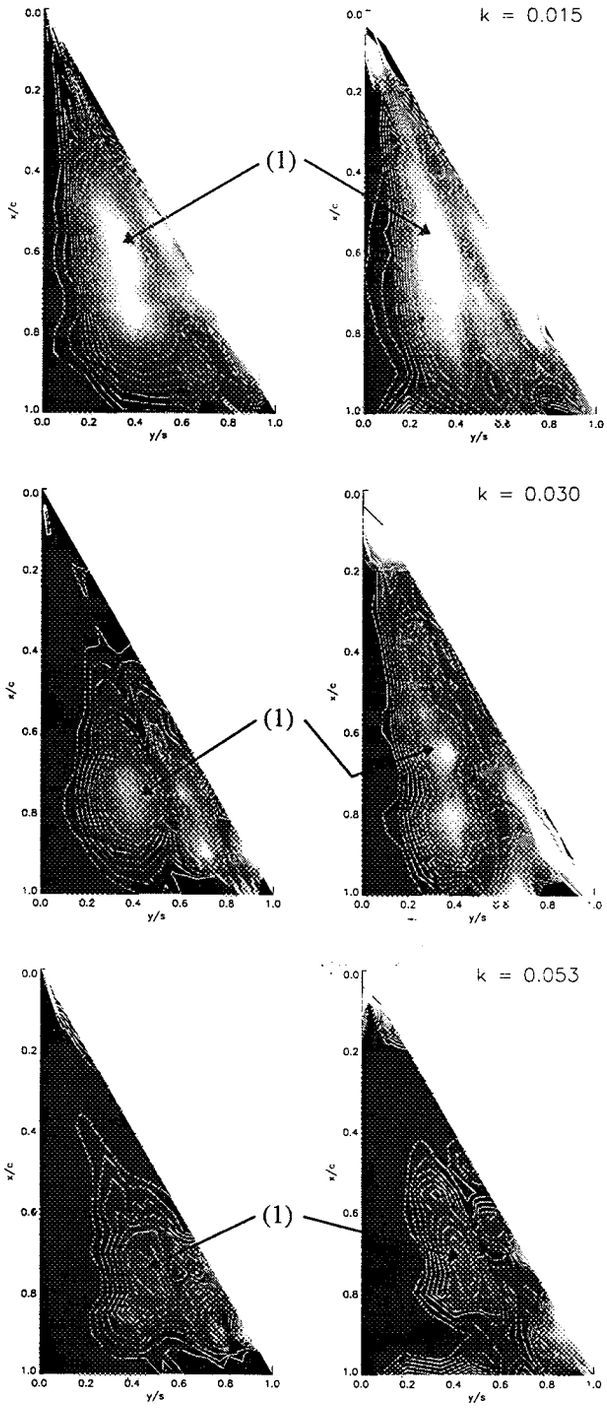

Figure 7 - RMS pressure distributions on two pitching delta wing planforms at 26° incidence

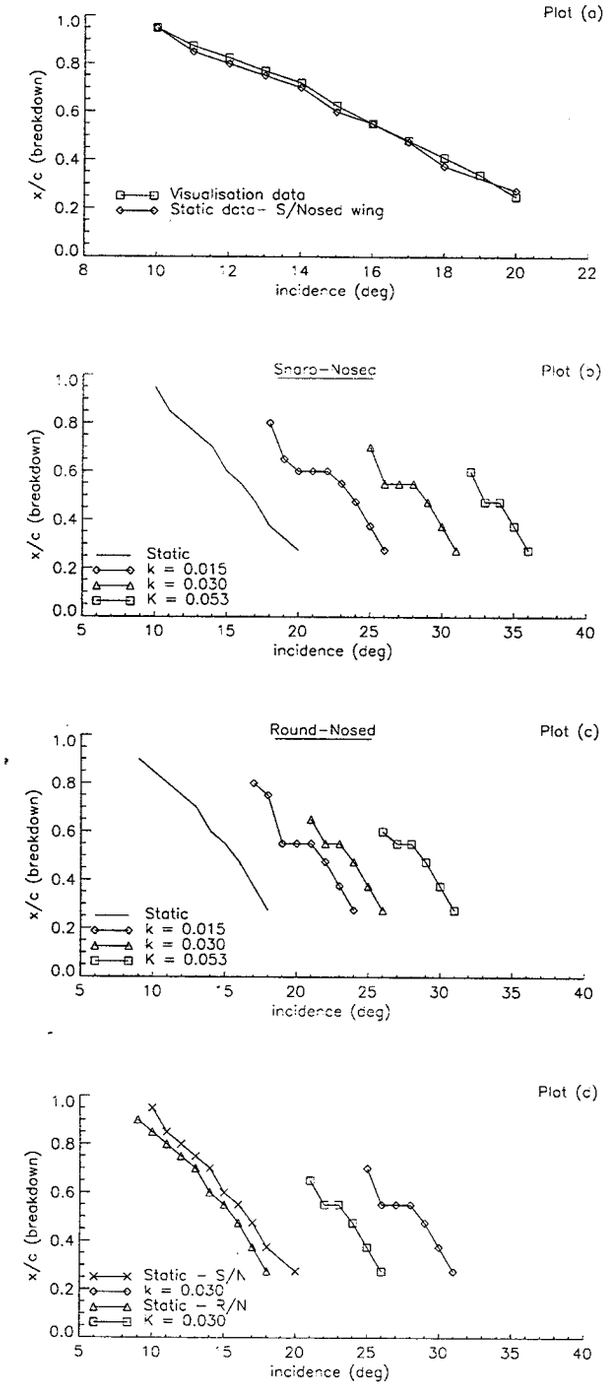

Figure 8 - Chordwise variation in vortex breakdown position for two delta wing planforms showing the effect of pitch rate & apex shape.

Figure 8 shows four plots of the chordwise location of vortex breakdown against angle of incidence. Plot (a) shows the similarity in behaviour of the vortex breakdown position determined by smoke visualisation data and the movement of the apex of the additional region of high RMS pressure identified in the analysis of the static pressure data for the sharp-nosed wing [17].

Discrepancies do occur very close to the apex of the wing and the trailing edge, the former due mainly to the poor pressure transducer density in this area compared with further down the wing (see Fig.1) and the latter due to the difficulties in pin-pointing the exact breakdown position so close to the trailing edge during the visualisation tests. Previous work [18] has identified significant delays in the movement of vortex breakdown on a delta wing (wing sweep angle = 59°) due to changes in reduced pitch rate during pitch up motions. Figure 8 plots (b) & (c) shows the position of the apex of the additional high RMS pressure region (Fig.6, location 1) against incidence for each wing at increasing reduced pitch rates. The trend apparent in the data shows delays in the movement of the additional region of high RMS pressure with increased pitch rate. Figure 8 plot (d) shows a comparison between the two wing configurations for the static case and for a single reduced pitch rate. These show a similarity in behaviour with the movement of breakdown as reported in the work of Miau et al [18]. The general trend indicates that the initial upstream movement of the additional peak of high RMS pressure occurs earlier on the round-nosed wing and that in both cases, there is a lack of uniformity of movement over the chord.

Discussion

The upper surface C_P distribution provides a clear indication of the position of the primary vortex core and its subsequent growth as the wing is pitched through a range of incidences. For the 60° wings tested in this study, the secondary vortices are not discernible. This observation is consistent with flow visualisation tests on the sharp-nosed wing [18] which revealed a small rotational velocity component in the secondary vortex structure throughout the incidence range. Similarly, the broadening and reduction in magnitude of the suction peak over the length of the vortex due to the conical nature of the flow structure, makes trailing-edge features, such as the arrival of vortex breakdown, difficult to detect.

Previous work [19] utilising off-body velocity measurements identified a region of high

turbulent kinetic energy above the surface of the wing inboard of the primary vortex core but outboard of the primary attachment zone. Similarly, two smaller regions of similar energy intensity were measured in areas which possibly correspond to the separation and reattachment zones of the secondary vortex. It is therefore likely that the primary region of high RMS pressure observed inboard of the vortex core is associated with a region of localised but highly turbulent flow within the feeding vortex sheet between the vortex core and the primary attachment region. Similarly, it is thought that the secondary region of high RMS pressures observed outboard of the vortex core is somehow associated with the formation of the secondary vortex structure.

It has been shown, for the static case, that there was a similarity between the vortex breakdown position determined by smoke visualisation and that obtained by analysis of sharp-nosed wing RMS pressure data. It was suggested that the waisting of the RMS pressure contours, highlighted in Figure 5 (3), and the associated localised trough of RMS pressure magnitude are indicative of the first subinterval of the breakdown region first described by Leibovich [20]. This subinterval is characterised by an axial deceleration of the approach flow and the formation of a stagnation point on the vortex axis. It is likely that the features evident in the RMS pressure distribution may be associated with an increase in the 'helix angle' of the vortex core velocity [21] during the deceleration phase. A change in the flow direction from that with a greater chordwise component to that with a predominantly spanwise component would align the flow more towards the surface normal direction at the primary reattachment point. The 'sharpening' of the angle of reattachment would then tend to reduce the RMS pressure 'footprint' immediately inboard of the reattachment point both in terms of magnitude and width.

As vortex breakdown develops, its arrival at the trailing edge of the wing and subsequently at chord stations upstream heralds a substantial increase in turbulent kinetic energy. This may in turn, be associated with the generation of a negative azimuthal component of vorticity. This was previously shown by Brown & Lopez [21] to be necessary for the axial component of velocity in the vortex core to be brought to rest and for vortex breakdown to take place. It has been shown that the development of negative azimuthal vorticity on a diverging stream surface that bounds the vortex core will induce a negative axial velocity on the vortex axis which, by continuity, will lead to a further divergence of the stream surface and a further increase in negative vorticity. It is suggested that it is this mechanism that is associated with the rapid increase in magnitude of the high RMS pressure region downstream of breakdown as well as the broadening of the region across the wing in a spanwise direction (Fig.5 (2)) as the wing incidence is increased.

In the pitch up cases, this expanded region of high RMS pressure, as show in Fig.7 at location (1), once again appears near the trailing-edge as the incidence increases. Unlike the static case however, there is no steady progression of this region towards the apex as the incidence is increased further. Rather, the region fluctuates in size before eventually expanding and moving towards the apex over a very short range of incidence. Similarly, the waisting of the RMS pressure contours immediately upstream of the region, witnessed in the static cases, is not apparent.

In a separate study of the pitching characteristics of the sharp-nosed wing [22], it was suggested that the initial appearance of the additional region of high RMS pressure on the wing is not a reliable indicator of the exact location of vortex breakdown. Examination of the progression of breakdown for the pitching cases presented in Figure 8 indicates that tracking this region produces breakdown histories which feature a distinct plateau region. This plateau corresponds to the period during which the additional region of RMS pressure maintains its position over the wing whilst fluctuating in size and implies that the forward movement is arrested at this point. Preliminary flow visualisation experiments, conducted as part of the present study, indicate that the initial movement of breakdown over the trailing-edge of the wing exhibits flow characteristics which are particularly complex and quite different from steady flow. The nature of progression of vortex breakdown from the trailing edge to the apex of the wing will be investigated in order that the physical nature of the plateau may be elucidated.

A principal effect of rounding the wing apex has been to move the origin of the peak suction region, associated with the primary vortex, from the apex of the wing to some point along the leading-edge. This has led to an increase in

the angle of the vortex path relative to the leading-edge when compared with its sharp-nosed counterpart. Figure 8 shows that there is a similarity in general behaviour between the sharp and round-nosed planforms in terms of the movement of the additional peaks of high RMS pressure. However, plot (d) indicates that for the round-nosed wing this occurs at a lower incidence. It is therefore suggested that the round-nosed wing experiences vortex breakdown over the wing at lower incidences both in the static and pitch up cases. Similarly, the speed of the upstream propagation of breakdown with incidence, as indicated by the RMS pressure distribution, is generally faster on the round-nosed wing.

Previous work by Lowson and Riley [23] has shown that the key effect in determining the vortex breakdown position on a wing with a given sweep angle is the apex shape. They suggested that the strength of vorticity shed near the apex of the wing is directly affected by variations in shape. The vorticity shed from the apex of the wing forms the centre of the vortex core, therefore any changes in apex geometry are bound to cause variations in the vorticity distribution at the centre of the core. It was also shown in work by Visser & Nelson [24] that there is a correlation between vorticity strength and wing sweep angle at a given angle of incidence. It is suggested in this case, that the rounding of the nose has the effect of reducing the effective sweep angle in the region of the wing apex and hence, reduces the strength of vorticity at the origin of the vortex core. This would have the effect of precipitating vortex breakdown.

Conclusions

Detailed experiments have been carried out on two pitching 60° delta wings with sharp leading-edges. The instantaneous and RMS pressure distributions on one half of the leeward surface of each wing has been successfully measured over an range of pitch rates, using a large number of closely spaced pressure transducers coupled to an advanced data acquisition system capable of sampling at a high rate. The capability to track vortex breakdown using the RMS pressure distribution has been demonstrated for the static case. Whilst this method provides useful information on the development of flow structures on the wing, its ability to track breakdown in the dynamic case is apparently limited by the manner in which breakdown is manifest over aft sections of the wing. It is suggested that the principal effect of rounding the wing nose is to reduce the effective sweep angle in the region of the wing apex which, in turn, reduces strength of vorticity at the origin of the vortex core.

Acknowledgements

The wind tunnel tests reported in this study were carried out with funding from the Engineering and Physical Sciences Research Council (EPSRC), GKN Westland Helicopters Ltd., the Defence Evaluation & Research Agency (DERA) and Glasgow University under contract GR/H48330. The authors also wish to acknowledge the additional support of the EPSRC through RS Quota award 96300150.

References

1. Lambourne, N.C. and Bryer D.W. (1961). "The bursting of leading-edge vortices - some observations & discussion of the phenomenon." Reports & Memoranda, No. 3282. Aero. Research. Council.
2. Elle, B.J. "On the breakdown at high incidences of the leading-edge vortices on delta wings." *J. Royal Aero. Soc.* (1960). **64.**(April): 491-493.
3. Gad-el-Hak, M. and Blackwelder R.F. "Control of the discrete vortices from a delta wing." *AIAA J.* (1987). **25.**(8): 1042-1049.
4. Lowson, M.V. "Visualisation measurements of vortex flows." *J. Aircraft* (1991). **28.**(5): 320-327.
5. Payne, F.M., Ng, T.T. and Nelson R.C. "Visualisation & flow surveys of the leading-edge vortex structure on delta wing planforms." AIAA Paper No. 86-0330. (1986).
6. Atta, R. and Rockwell D. "Hysteresis of vortex development and breakdown on an oscillating delta wing." *AIAA J.* (1987). **25.**(11): 1512-1513.
7. Gad-el-Hak, M. and Ho C.-M. "The pitching delta wing." *AIAA J.* (1985). **23.**(11): 1660-1665.
8. Gad-el-Hak, M. and Ho C.-M. "Unsteady vortical flow around three-dimensional lifting surfaces." *AIAA J.* (1986). **24.**(5): 713-721.
9. LeMay, S.P., Batill, S.M. and Nelson R.C. "Vortex dynamics on a pitching delta wing." *J. Aircraft* (1990). **27.**(2): 131-138.
10. Wolffelt, K.W. "Investigation on the movement of vortex burst position with

dynamically changing AoA for a schematic deltawing in a water tunnel with correlation to similar studies in a windtunnel." AGARD CPP 413 (1986). AGARD.

11. Gursul, I. and Yang H. "Vortex breakdown over a pitching delta wing." *J. fluids & structures* (1995). **1995**. (9): 571-583.
12. Rediniotis, O.K., Klute, S.M., Hoang, N.T. and Telionis, D.P et al. "Dynamic pitch up of a delta wing." *AIAA J.* (1994). **32.**(4).: 716-725.
13. Thompson, S.A., Batill, S.M. and Nelson R.C. "Delta wing surface pressures for high angle of attack manoeuvres." AIAA Paper No. 90-2813. (1990).
14. Parker, A.G. "Aerodynamic characteristics of slender wings with sharp leading edges - A review." *J. Aircraft* (1976). **13.**(3): 161-168.
15. Jarrah, M.A.M. "Visualisation of the flow about a delta wing manoeuvring in pitch to very high angle of attack." *ASME (Fluids Engineering Division) Publication FED,* (1990). **92** : 109-116.
16. Woods, M.I. and Wood N.J. "Unsteady aerodynamic phenomena on novel wing planforms." ICAS Paper No. ICAS-96-2.11.2 (1996).
17. Jupp, M.L., Coton F.N. and Green R.B. "A statistical analysis of surface pressure measurements with particular reference to vortex breakdown." Glasgow University Aero Report No. 9806. (1998).
18. Miau, J.J., Chang, R.C., Chou, J.H. and Lin, C.K. "Non-uniform motion of leading-edge vortex breakdown on ramp-pitching delta wings." *AIAA J.* (1992). **30.**(7): 1691-1702.
19. Honkan, A. and Andreopoulous. J. "Instantaneous three-dimensional vorticity measurements in vortical flow over a delta wing." *AIAA J.* (1997). **35.** (10):1612-1620.
20. Leibovich, S. "The structure of vortex breakdown." *Ann. Review Fluid Mech.* (1978). **10.**: 221-246.
21. Brown, G.L. and Lopez J.M. "Axisymmetric vortex breakdown, Part 2 - Physical mechanisms." *J. Fluid Mech* (1990). **221** : 553-576.
22. Jupp, M.L., Coton F.N., Green R.B. and Galbraith R.A.McD. "An analysis of a pitching delta wing using high resolution pressure measurements." AIAA Paper No. 98-2743. (1998).
23. Lowson, M. and Riley, A. J. "Vortex breakdown control by delta wing geometry." *J. Aircraft* (1995) **32.** (4): 832-838.
24. Visser, K.D. and Nelson R.C. "Measurements of circulation & vorticity in the leading edge vortex of a delta wing." *AIAA J.* (1993). **31.**(1): 104-111.